THIS DOCUMENT IS PROTECTED BY U.S. AND INTERNATIONAL COPYRIGHT
It may not be reproduced, stored in a retrieval system, distributed or transmitted, in whole or in part, in any form or by any means.
Downloaded from SAE International by Jaguar Cars Ltd, Thursday, August 08, 2013 09:15:34 AM

SAE International™

The Effects of Unsteady On-Road Flow Conditions on Cabin Noise: Spectral and Geometric Dependence

2011-01-0159
Published
04/12/2011

Nicholas R. Oettle, David Sims-Williams and Robert Dominy
Durham Univ.

Charles Darlington and Claire Freeman
Jaguar Land Rover

Copyright © 2011 SAE International

doi:10.4271/2011-01-0159

ABSTRACT

The in-cabin sound pressure level response of a vehicle in yawed wind conditions can differ significantly between the smooth flow conditions of the aeroacoustic wind tunnel and the higher turbulence, transient flow conditions experienced on the road. Previous research has shown that under low turbulence conditions there is close agreement between the variation with yaw of in-cabin sound pressure level on the road and in the wind tunnel. However, under transient conditions, sound pressure levels on the road were found to show a smaller increase due to yaw than predicted by the wind tunnel, specifically near the leeward sideglass region.

The research presented here investigates the links between transient flow and aeroacoustics. The effect of small geometry changes upon the aeroacoustic response of the vehicle has been investigated. It was found that sideglass pressures showed close agreement at all turbulence levels while surface sound pressure levels also showed similar behaviour under a wide range of on-road flow conditions. While the overall sideglass sound pressure level changed under the various yaw conditions, the change in shape of the frequency spectrum was less significant.

Geometry changes made to a base vehicle reduced the sensitivity of the in-cabin noise to on-road turbulence, showing that shape-change can modify sensitivity to on-road turbulence.

INTRODUCTION

At higher vehicle speeds, aerodynamic noise tends to dominate the overall noise level inside the passenger compartment of a vehicle. At speeds that are commonly attained on a highway, aerodynamic noise dominates, as shown by Hucho (1998) [1] and Blumrich (2009) [2]. As the level of tyre, engine and powertrain noise have reduced as vehicles have developed, the relative importance of aerodynamic noise has increased. This is particularly the case in the luxury vehicle sector, where these other sources are more isolated from the passengers. In addition, primary noise generation sources such as the A-pillar region, Watkins (1999) [3], and door mirrors, George (1990) [4], tend to be located very close to the driver and therefore the driver is very sensitive to noise produced in these regions. With the emergence of new technologies such as electric vehicles, aerodynamic noise will become increasingly important owing to the consequent reduction in engine noise.

As the automotive industry develops vehicles with increased fuel efficiency and reduced emissions, the overall level of comfort inside a vehicle remains important as a differentiator between vehicles. Cabin noise is an important component of the passenger experience inside a vehicle and it follows that aerodynamic noise is therefore linked to how a customer perceives the overall levels of comfort and quality of a particular vehicle.

Being able to predict how a vehicle will behave in the transient, turbulent conditions experienced on-road during the development of a vehicle is important, since changes in

THIS DOCUMENT IS PROTECTED BY U.S. AND INTERNATIONAL COPYRIGHT
It may not be reproduced, stored in a retrieval system, distributed or transmitted, in whole or in part, in any form or by any means.
Downloaded from SAE International by Jaguar Cars Ltd, Thursday, August 08, 2013 09:15:34 AM

design due to yaw and turbulence sensitivity can become very costly later in the design process. Typically, aerodynamic noise development work takes place in an aeroacoustically treated wind tunnel that, in the majority of cases, has flows that are both spatially and temporally invariant. The noise generated in these steady flows are correspondingly steady and therefore do not fully capture the vehicle's response to the unsteady flows typically experienced on-road. Turbulence generation systems have been installed in aeroacoustic wind tunnels as shown Cogotti (2003, 2005) [5] [6], which can be used to assess cabin noise under these turbulent conditions. Passive systems, such as those placing a vehicle upstream of the test section as described by Saunders and Mansour (2000) [7], Watkins et al. (2001) [8], Cogotti (2003) [5] amongst others, tend to simulate only a limited range of conditions that a vehicle can experience while traversing the on-road environment. Active methods allow a wider range of conditions to be simulated and as these methods improve, better comparisons can be made between the on-road environment and the aeroacoustic wind tunnel. However, the full range of conditions that a vehicle can experience, as investigated by Wordley and Saunders (2008, 2009) [9] [10], are still not possible to fully simulate.

Alternatively, simulation techniques such as those described by Krampol et al. (2009) [11] can avoid the use of such turbulent simulation devices. Using these techniques, cabin noise is recorded under a range of flow velocities and yaw angles and blended together based on typical on-road conditions. However, these techniques are currently limited by the assumption that the cabin noise response is quasi-steady and unaffected by the faster transient conditions experienced on-road.

A small number of studies have taken place including those by Watkins et al. (2001) [8] and Lindener et al. (2007) [12], comparing the cabin noise response of a vehicle on-road and in the aeroacoustic wind tunnel. Previous work by Oettle et al. (2010) [13] has shown that on-road, the cabin noise can vary in level from that predicted by the aeroacoustic wind tunnel. It was found that the variation of in-cabin sound pressure level (SPL) with yaw in the wind tunnel was in close agreement with on-road data at low lateral turbulence intensities. However, at higher lateral turbulence intensity there was a discrepancy between the wind tunnel and on-road sound pressure level, specifically to noise levels near the leeward sideglass. Sound pressure levels in this area were shown to have a smaller increase due to yaw than predicted by the aeroacoustic wind tunnel, indicating that transient flows around the leeward side of the vehicle may not have time to fully develop to their steady, high SPL condition.

Lawson et al. (2007, 2008) [14] [15] investigated differences in flow structures of a vehicle on-road and in the wind tunnel, particularly in the A-pillar region. This paper aims to investigate this further by assessing how flow structures and noise generation around the sideglass region are affected by variations in yaw angle and turbulence on-road. In addition to how the overall level of the cabin noise varies under on-road conditions, changes to the frequency content of the cabin noise were assessed. Finally, the effects of minor geometry changes to the vehicle were evaluated within the on-road environment.

EXPERIMENTAL METHOD

TEST VEHICLE AND BODY MODIFICATIONS

A European luxury saloon was used as the test vehicle, shown in Figure 1. The coordinate system that is used throughout the paper is shown in Figure 2, when viewed from above the vehicle. The probe is aligned with the vehicle throughout the experimentation.

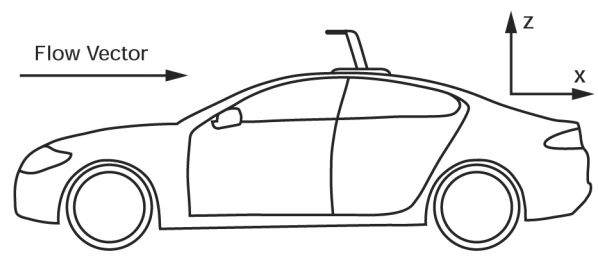

Figure 1. Test vehicle showing location of probe

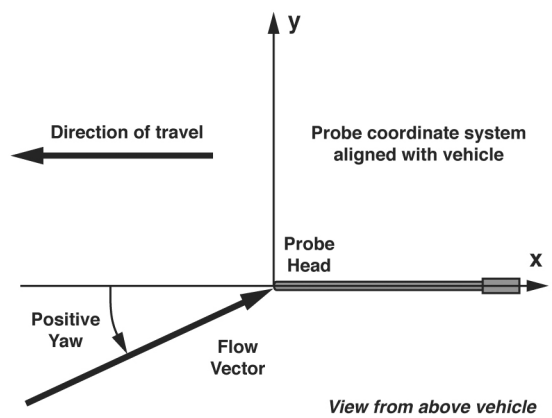

Figure 2. Probe and vehicle coordinate system

The base vehicle was the same as used in previous work described by Oettle et al. (2010) [13], with modifications made to both the door mirror housing and bonnet. The stems of the door mirrors were modified to improve subjective cabin noise performance, as shown in Figure 3. To reduce the effect of the windscreen wipers on noise generation, a modification to the rear lip of the bonnet was also tested. Such a deflector to reduce the effect of the windscreen wipers on the cabin noise is described by Zaccariotto et al. [16]. Rapid-prototype material sections were used to increase the

THIS DOCUMENT IS PROTECTED BY U.S. AND INTERNATIONAL COPYRIGHT
It may not be reproduced, stored in a retrieval system, distributed or transmitted, in whole or in part, in any form or by any means.
Downloaded from SAE International by Jaguar Cars Ltd, Thursday, August 08, 2013 09:15:34 AM

height of the bonnet lip so that a larger proportion of the wipers were shielded from the oncoming flow. The sections were blended into the existing contours of the bonnet using modelling clay and secured using adhesive tape. The resulting bonnet kicker increased the height of the rear lip and 'power bulge' of the bonnet by approximately 15 mm, terminating at the trailing edge with a vertical face. This is shown in Figure 4, with a summary of the geometry modifications shown in Table 1.

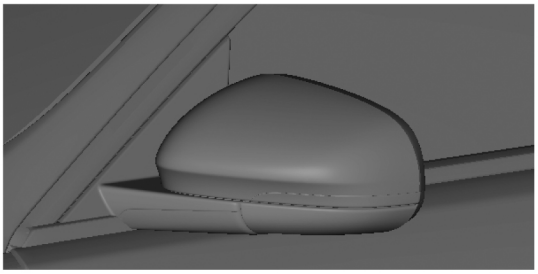

(a). Geometry 1

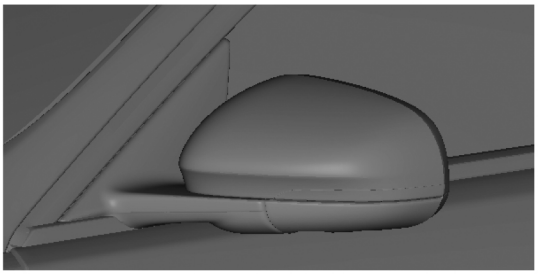

(b). Geometries 2 and 3

Figure 3. Details of mirror modifications

Figure 4. Geometry 3 bonnet kicker

Table 1. Summary of geometry modifications and naming scheme

Name	Description
Geometry 1G	Base vehicle
Geometry 2G	As Geometry 1G, but with modified door mirror housing
Geometry 2	As Geometry 2G, but with surface microphones and Perspex sideglass for pressure measurements
Geometry 3G	As Geometry 2G, but with addition of bonnet kicker
Geometry 3	As Geometry 3G, but with surface microphones and Perspex sideglass for pressure measurements

FLOW MEASUREMENT

To measure the flow over the vehicle, a roof-mounted 5-hole probe was used. The probe was manufactured and calibrated in isolation using facilities at Durham University. Yaw angles and other quantities reported are therefore the actual values at the probe location. This approach avoids embedding the steady state response of the vehicle (for example, a local velocity increase at the probe) in the probe calibration. This is important since this investigation concerns the comparison between the aerodynamic response of the vehicle under steady state and transient conditions. Positioning the probe ahead of the vehicle, such as in the work by Wordley and Saunders (2008, 2009) [9] [10], would reduce the influence of the vehicle's body on the flow measurements, but would alter the flow around the vehicle. The small size of the probe head is important, since it is this size that limits the response of the probe. Since this paper is concerned about measuring the response of the vehicle to oncoming transient conditions, it is necessary for the probe to be smaller than the vehicle to have a flat response to these conditions in situations where the vehicle may not.

Five SensorTechnics HCLA12X5DB pressure transducers were used to measure the probe pressures. These measure differential pressure and have a range of ±12.5 mbar. The transducers were packaged into a single enclosure with a common reference and located within the probe mounting. The reference port was connected via a PVC tube to a location in the trunk of the vehicle. The probe mounting was attached to the roof of the vehicle magnetically. Wind tunnel testing confirmed that the induced noise of the probe was small when measured from inside the vehicle.

The probe tip was positioned approximately 320 mm above the vehicle's roofline, and approximately 70 mm in front of the B-pillar, as shown in Figure 1. This position was consistent for each of the on-road tests.

THIS DOCUMENT IS PROTECTED BY U.S. AND INTERNATIONAL COPYRIGHT
It may not be reproduced, stored in a retrieval system, distributed or transmitted, in whole or in part, in any form or by any means.
Downloaded from SAE International by Jaguar Cars Ltd, Thursday, August 08, 2013 09:15:34 AM

To measure the pressure distribution around the A-pillar region, a Perspex sideglass of the same size as the original glass was used. This was positioned on the driver's side (front right) of the vehicle. The exterior pressure was measured at ten locations as shown in Figure 5. Each of these locations were drilled and 10 mm lengths of 1.24 mm OD tubing bonded in position, ensuring the outer surface of the sideglass remained smooth. The tubing inserts were connected to ten SensorTechnics HCLA12X5DB pressure transducers located inside the cabin via PVC tubing. Pressures were measured relative to trunk pressure, although pressure coefficients were defined based on vehicle velocity and static pressure measured at the probe tip.

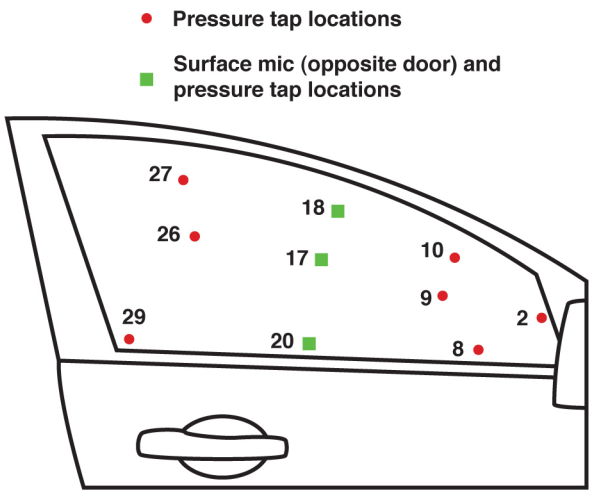

Figure 5. Location of pressure tappings and surface microphones

A probe and tubing transfer function correction was applied, for magnitude and phase, to all on-road data for both the roof mounted five-hole probe and the sideglass pressure tappings. This is described by Irwin et al. (1979) [16] and developed by Sims-Williams and Dominy (1998) [18]. Similar examples of its application are shown by Lawson et al. (2007) [14]. With the probe and remote transducers used in the investigation, this approach allows a frequency response in excess of 500 Hz. This significantly exceeds the required response for this application, since the energy contained within higher frequencies is low (three orders of magnitude lower at 500 Hz when compared to 1 Hz), as shown by Wordley (2009) [10]. The higher frequency fluctuations contained in the wind are also correspondingly small and are therefore not correlated over the scale of the vehicle.

DATA ACQUISITION

To log the output from the pressure transducers, a National Instruments NIDAQmx USB-6218 data logger was used. This was controlled by a laptop running control software developed at Durham University. Data were also received from a Bluetooth GPS device that was simultaneously logged with the pressure transducer data from the data logger using the same control software. The GPS data included details of the velocity and heading of the vehicle, in addition to information on the location of the vehicle and time of the experiment. The pressure transducer data were logged in sets of 16384 points at 500 Hz, therefore giving a logging duration of 32.768 s. This logging time was considered suitable to capture the transient nature of the on-road environment. To reduce aliasing, the signal from each of the pressure transducers was passed through a 250 Hz second-order low-pass filter.

The data logging system included a number of features to assist with the correlation between the data and the on-road environment, as well as the in-vehicle control of the system. An LED display was mounted on the dashboard of the vehicle, providing the driver with information on the logging status, GPS signal and run number. A video camera also recorded on-road events to further assist correlation between the external environment and the flow and noise data. To synchronise both the flow and audio logging systems, a combined external trigger was used to start both systems from within the vehicle. A schematic of the entire logging system is shown in Figure 6.

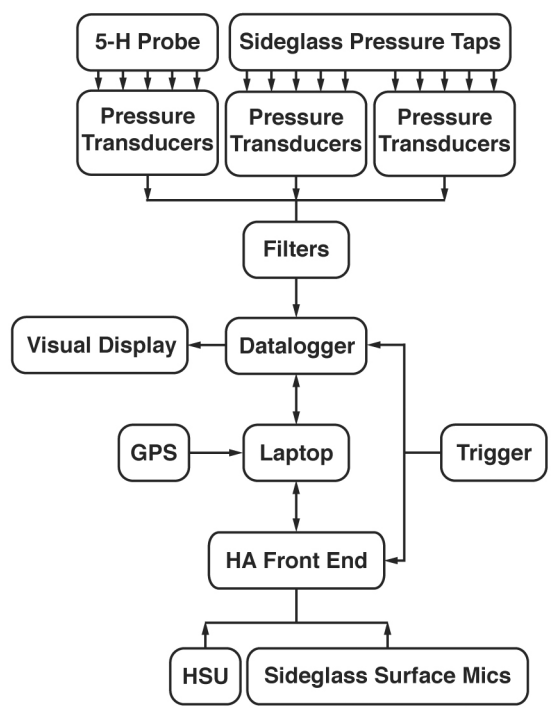

Figure 6. Schematic of logging system

NOISE MEASUREMENT

A Head Acoustics HSU (head and shoulder unit, or acoustic head) with torso was used to record the cabin noise. The HSU was positioned on the front left (passenger) seat of the vehicle and fixed securely to prevent any additional noise generation.

THIS DOCUMENT IS PROTECTED BY U.S. AND INTERNATIONAL COPYRIGHT
It may not be reproduced, stored in a retrieval system, distributed or transmitted, in whole or in part, in any form or by any means.
Downloaded from SAE International by Jaguar Cars Ltd, Thursday, August 08, 2013 09:15:34 AM

The ventilation system was switched off during testing. Since the noise data recorded by the acoustic head would be affected by the presence of the Perspex sideglass and surface microphones, cabin noise data is only presented with glass sideglass and no surface microphone measurements.

To measure the noise on the surface of the vehicle, three B&K 4949 10 mm surface microphones were used. These were positioned on the passenger sideglass in positions corresponding to three of the surface pressure tappings on the opposite (driver's side) sideglass, as shown by Figure 7. Aluminium adhesive tape was used to attach the microphones to the surface of the sideglass, shown in Figure 7. Cables entered the vehicle through the lower door seal.

Simultaneously logging surface noise and pressure on opposite sides of the vehicle has the advantage of allowing both noise and pressure data to be collected in broadly similar on-road flow conditions, when compared to collecting data in two discrete periods. This is particularly the case when back-to-back runs were collected on the same section of road, as was during this testing. However, this has the disadvantage of the results being coloured by any asymmetry in the vehicle and therefore care must be taken when assessing correlations between surface pressure and surface noise.

Figure 7. Detailed view of surface microphone attachment

Both the HSU and surface microphones were connected to the logging computer via a Head Acoustics front-end and controlled through the Head Acoustics HEAD Recorder software. Logging took place at 44.1 kHz. In addition to the combined trigger for both flow and audio logging systems, a 2 kHz tone was generated and silenced at the point of logging to assist synchronising the logging systems with the digital camera.

Head Acoustics ArtemiS software was used to extract SPL (sound pressure level) from the audio data collected both on-road and in the wind tunnel. When calculating the SPL, an integration time of 2 ms was chosen to match the time period over which the data logger recorded the flow data.

WIND TUNNEL TESTING

The vehicle was tested in the three-quarter open aeroacoustic wind tunnel (AWT) in the Ford Merkenich Technical Centre, Cologne. Turbulence intensity in the x and y directions was less than 0.5%. Cortex MK1 heads were placed in the vehicle. These heads have a slightly different transfer function to the Head Acoustics head used during on-road testing. However, the resulting impact on measured cabin noise spectrum is small compared with the differences in spectrum between the AWT and on-road. As with on-road testing, the ventilation system was switched off. The vehicle was yawed in stages of 0, 2, 4, 6, 8, 10 and 20 degrees, in both positive and negative directions.

ROAD TESTING

Road testing took place on divided highways, corresponding to those used in [13]. The road surface included both hot-rolled and coarse chip asphalt, as typically experienced by a vehicle. The vehicle speed matched the wind tunnel velocity. The on-board cruise control was used to keep a consistent speed, although the GPS was used to determine an accurate velocity. A variety of wind conditions were chosen in order to capture the range of yaw angles that would be experienced on the road. These included high-yaw conditions experienced during particularly windy days. Traffic conditions were varied during the course of experimentation, although data collection was usually performed in light traffic as it was in these conditions that a constant speed could be most frequently held. Data collected during runs where a constant speed was not held were discarded. In addition to passing vehicles, a range of different roadside obstacles were encountered during data collection including crash barriers, trees, signs and bridges as shown in Figure 8. Where possible, tests with different geometries were carried out on the same day, so that the range of conditions experienced for all test cases were as similar as possible.

Figure 8. Typical on-road conditions

THIS DOCUMENT IS PROTECTED BY U.S. AND INTERNATIONAL COPYRIGHT
It may not be reproduced, stored in a retrieval system, distributed or transmitted, in whole or in part, in any form or by any means.
Downloaded from SAE International by Jaguar Cars Ltd, Thursday, August 08, 2013 09:15:34 AM

RESULTS

COORDINATE SYSTEM

Figure 9 shows a summary of the coordinate system used throughout experimentation. When the vehicle is subject to oncoming flow with negative yaw, the acoustic head and surface microphones are in the leeward region, whereas the pressure tappings are in the windward region. Conversely at positive yaw, the opposite situation applies.

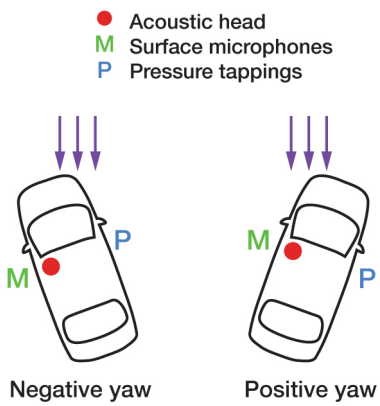

Figure 9. Summary of coordinate system used showing location of acoustic head

ON-ROAD CONDITIONS

Figure 10 shows the distribution of oncoming flow yaw angles experienced by the vehicle during experimentation. For both fully instrumented vehicle configurations, the yaw angle is confined to a range between ± 20 degrees, with a bias towards positive yaw angles owing to the wind conditions experienced during the period of testing.

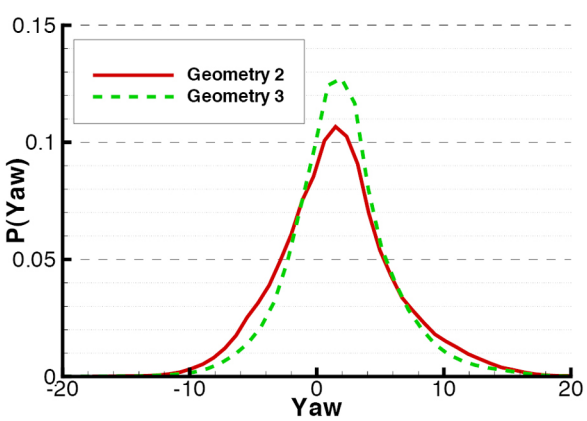

Figure 10. Yaw probability distribution

From the data collected by the roof-mounted probe, details of the oncoming flow turbulence were determined. Component turbulence intensity for a single vehicle geometry in both the *x* and *y* directions is shown in Figure 11, plotted against bulk turbulence intensity. A rolling window of 2048 samples (approximately 4 seconds duration) was used to determine the turbulence conditions. Using the reduced frequency criteria as described by He (1996) [19], this window is sufficiently large to capture all non-quasi-steady events.

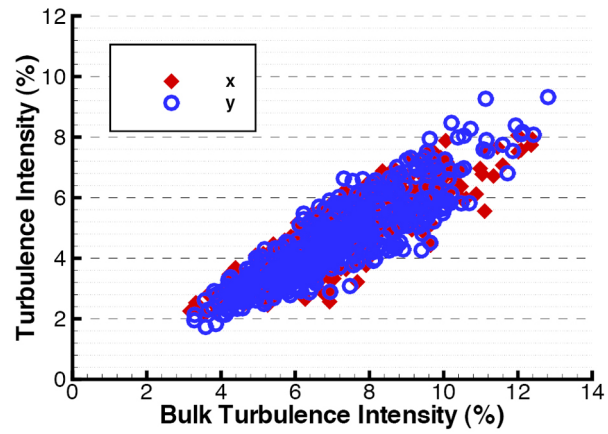

Figure 11. Component turbulence intensity vs. bulk turbulence intensity (Geometry 2)

The turbulence conditions experienced by both vehicle configurations were similar. In addition, the turbulence intensity is comparable to that reported previously by Wordley (2009) [10] and also to Lindener et al. (2007) [12].

DATA PROCESSING

To assist in the interpretation of the fluctuating on-road data, an averaging process was adopted. For a particular variable or set of variables (for example *yaw* as shown in Figure 12) the instantaneous values are grouped into a series of discrete bins. The average of other variables within each bin was then determined, providing insight into the overall behaviour of the variables under a range of different conditions. In this paper, bins based on flow yaw angle alone, and yaw angle and *y*-component turbulence intensity are presented.

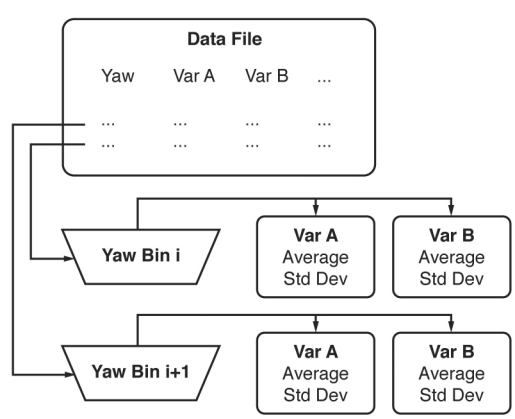

Figure 12. Schematic of bin average method

THIS DOCUMENT IS PROTECTED BY U.S. AND INTERNATIONAL COPYRIGHT
It may not be reproduced, stored in a retrieval system, distributed or transmitted, in whole or in part, in any form or by any means.
Downloaded from SAE International by Jaguar Cars Ltd, Thursday, August 08, 2013 09:15:34 AM

SIDEGLASS DATA

Figure 13 shows the variation in pressure coefficient with yaw and turbulence intensity at two locations on the sideglass of vehicle Geometry 2. Turbulence intensity is a convenient measure of rate of change of yaw angle. Point 18 was close to the A-pillar and Point 20 was near the base of the sideglass, as shown in Figure 5. Both points show an increase in pressure at negative (windward) yaw, when the oncoming flow impinges onto the sideglass. When the sideglass is at the leeward side, at positive yaw, Point 18 shows more sensitivity towards yaw than Point 20. The point closest to the A-pillar is likely to be more affected by changes in the A-pillar vortex with yaw, than the point at the base of the sideglass. Data at both points for different rates of change of yaw angle collapse onto a single characteristic. This agrees with Lawson (2008) [15] whereby the pressures around the A-pillar region were in close agreement both on-road and in the wind tunnel.

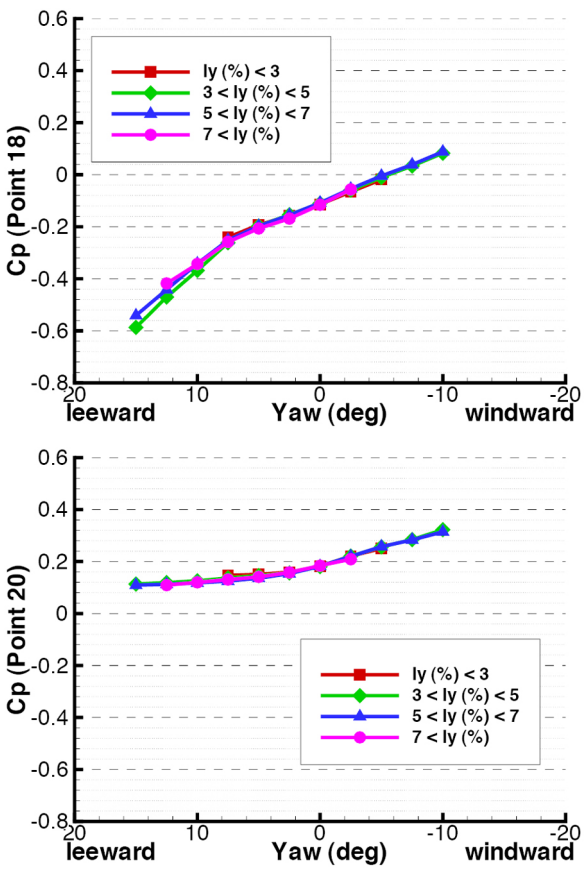

Figure 13. Sideglass pressure under turbulence conditions (Geometry 2)

To compare the effects of changes in geometry, specifically between Geometries 2 and 3, the sensitivity of Points 18 and 20 towards yaw are shown in Figure 14. This figure shows the overall yaw response to all levels of turbulence experienced on-road. Geometry 3 shows very similar behaviour to Geometry 2 at all yaw angles, with a slight deviation under the more extreme yaw conditions. At positive yaw, the sideglass will be in the leeward region, after the flow has had the opportunity to intersect with the windscreen wipers, which may explain the deviation between the two geometries at high positive yaw. However, this effect is relatively small and shows that the effects of the wipers and bonnet kicker in the sideglass region to be slight.

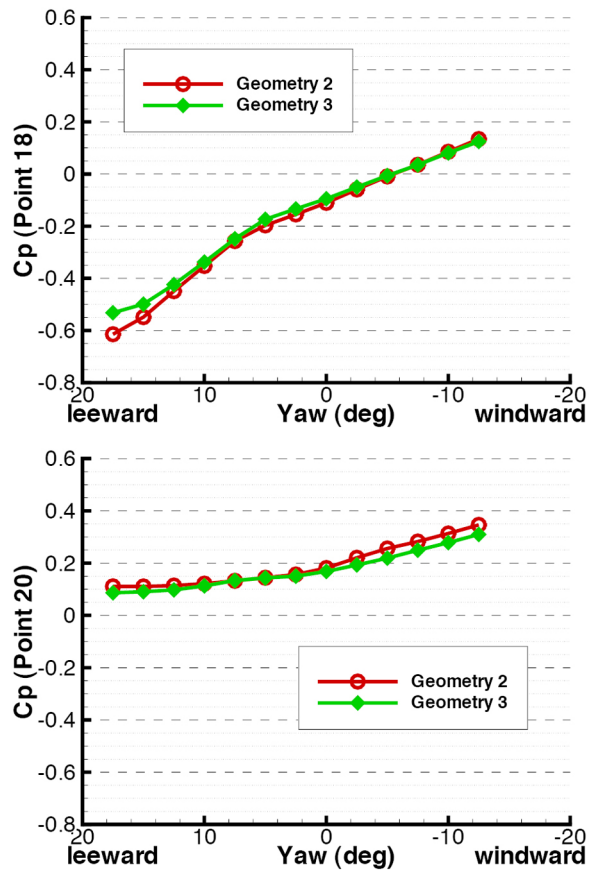

Figure 14. Comparison of sideglass pressure between vehicle geometries

To compare how both pressure and SPL are affected by yaw and turbulence, Figure 15 shows pressure and SPL at Point 18 of vehicle Geometry 2. Since it is not possible to record pressure and SPL simultaneously at the same point, surface microphones and pressure tappings were located in the same position on opposite doors. These are then plotted together, with the yaw axis of the pressure graph reversed, so that at each point directly above each other, both locations will either be in a leeward or windward position. Asymmetry in the vehicle, such as the windscreen wipers and slight changes in the door mirror angle will result in these opposite points not being entirely equivalent. The sideglass is in the leeward region on the left side of the graphs, changing towards a windward position as one follows the graph to the right.

THIS DOCUMENT IS PROTECTED BY U.S. AND INTERNATIONAL COPYRIGHT
It may not be reproduced, stored in a retrieval system, distributed or transmitted, in whole or in part, in any form or by any means.
Downloaded from SAE International by Jaguar Cars Ltd, Thursday, August 08, 2013 09:15:34 AM

In the leeward region, there is increased noise generation owing to the separated flow structures present. The increased levels of turbulence result in more noise production, as shown by Watkins (1999) [3]. Conversely, as the sideglass moves into a windward position, noise generation decreases. There is a larger spread in SPL than in pressure data. This is likely to be caused by other varied noise sources not correlated with yaw being detected by the surface microphones.

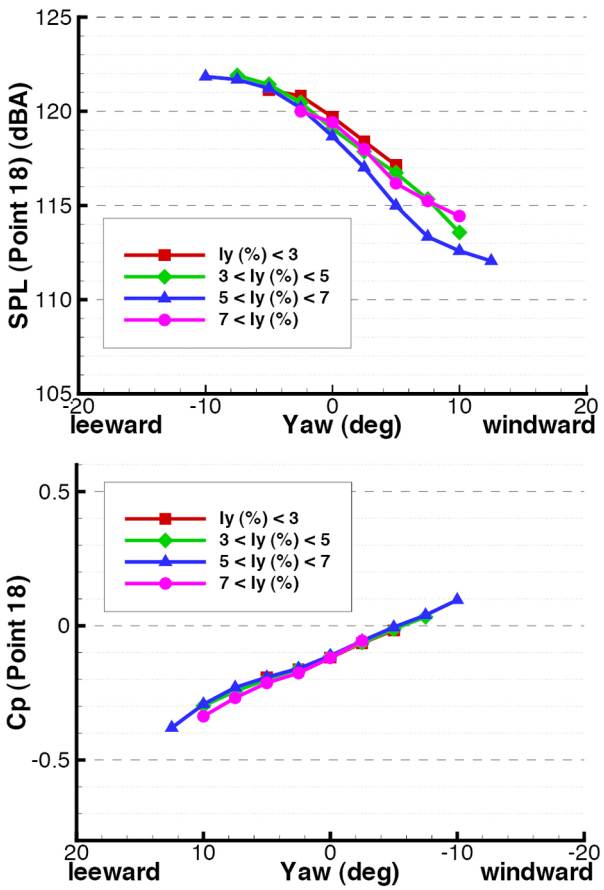

Figure 15. Comparison of sideglass pressure and SPL under different turbulence conditions (Geometry 2)

Figure 16 shows the same comparison between SPL and pressure for vehicle Geometry 3. The overall behaviour of Geometry 3 is similar to Geometry 2, with a slight overall increase in overall SPL and the sensitivity of the SPL towards yaw. However, the behaviour of sideglass SPL follows the same overall behaviour of sideglass pressure, in that it is not significantly affected by the windscreen wipers.

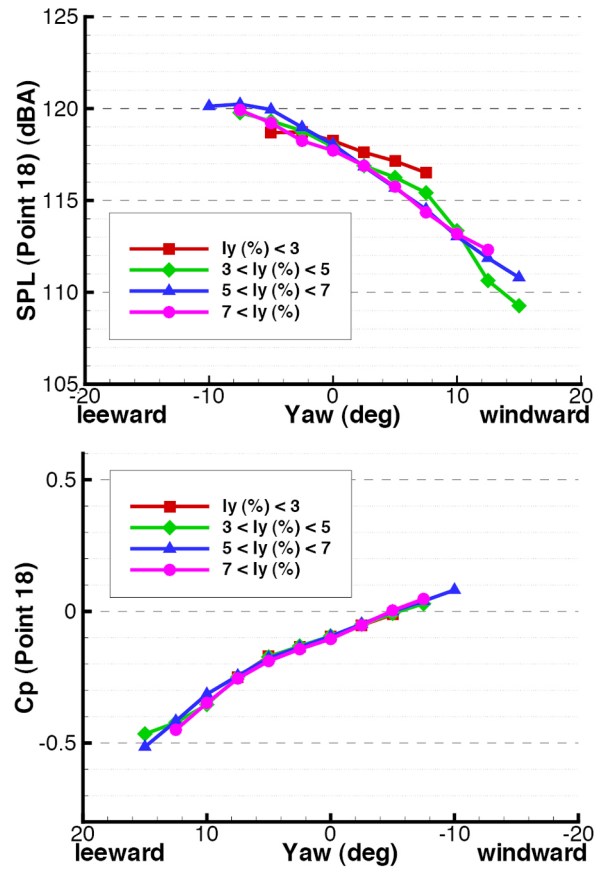

Figure 16. Comparison of sideglass pressure and SPL under different turbulence conditions (Geometry 3)

The transient conditions experienced on-road produce both amplitude and frequency modulation to the noise experienced inside the cabin and it is useful to assess the relative importance of these two effects. To compare how the spectral content of the SPL measured at Point 18 varies with yaw angle, Figure 17 shows the variation of the third octave spectrum with yaw. As shown by the overall SPL in Figure 15, as the flow around the sideglass becomes more separated at negative yaw, noise generation increases. What Figure 17 shows is that while the overall SPL varies with yaw, the spectrum shape remains unchanged, indicating that changes in amplitude of the noise are more significant than in changes in frequency.

THIS DOCUMENT IS PROTECTED BY U.S. AND INTERNATIONAL COPYRIGHT
It may not be reproduced, stored in a retrieval system, distributed or transmitted, in whole or in part, in any form or by any means.
Downloaded from SAE International by Jaguar Cars Ltd, Thursday, August 08, 2013 09:15:34 AM

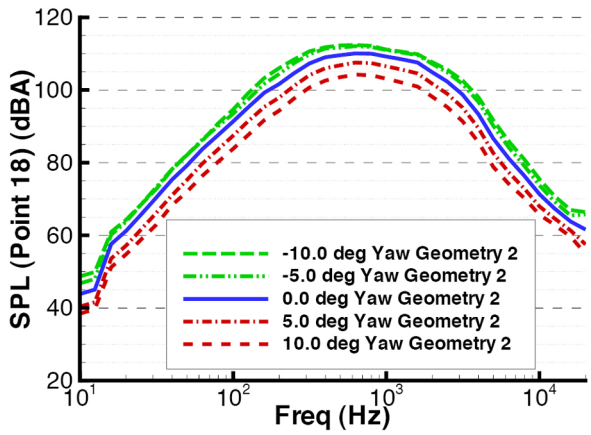

Figure 17. Third octave spectrum of sideglass SPL under different yaw conditions (Geometry 2)

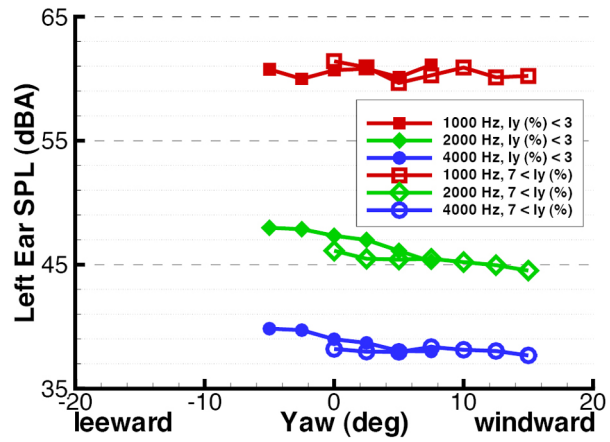

Figure 19. Selected third octave frequency bands under different yaw and turbulence conditions (Geometry 2G)

IN-CABIN NOISE

Figure 18 shows how selected frequencies of cabin noise vary with yaw angle. Three third-octave frequency bands were chosen which are particularly relevant to an occupant in the cabin. The overall (frequency independent) variation of SPL with yaw is shown in Figure 20. Each frequency band behaves in a similar manner, increasing in level at negative yaw angle.

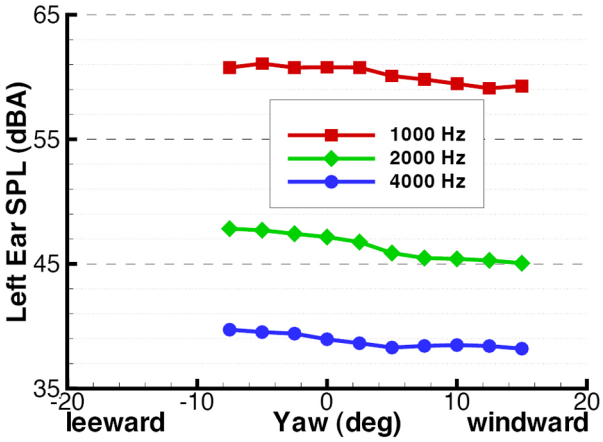

Figure 18. Selected third octave frequency bands under different yaw conditions (Geometry 2G)

To isolate the response of each of the frequency bands to different levels of on-road yaw fluctuation, Figure 19 shows the same data but split into regions of both high and low turbulence. Data collected under different conditions of yaw fluctuation collapse onto a single characteristic, reinforcing the concept that changes in overall level of cabin noise are more important than changes in frequency under different on-road conditions.

Figure 20 shows the variation of cabin SPL in both the AWT and under different levels of on-road turbulence for vehicle geometries 1G and 2G, comparing the effect of the two mirror designs on cabin noise. The AWT data show a lower cabin noise than the data collected on-road, where the shift in level is attributed to additional noise generation sources, such as the tyre and engine noise present on-road but not in the AWT.

Under the steady, low turbulence conditions of the AWT, the Geometry 1G and 2G vehicles show similar behaviour under the same yaw conditions, with the Geometry 2G vehicle having consistently lower cabin noise than the Geometry 1G vehicle. This contrasts with the behaviour under the lower turbulence conditions experienced on-road, where the Geometry 2G vehicle shows a slightly increased cabin noise when compared to the Geometry 1G vehicle. However, under higher levels of turbulence, the Geometry 1G vehicle has increased cabin noise over the Geometry 2G vehicle. In addition, the cabin noise response of both vehicles on-road does not show the same symmetrical behaviour under windward and leeward conditions as the response in the AWT.

The cabin noise response of both vehicle geometries to lower levels of turbulence is similar, with the Geometry 1G vehicle having a slightly quieter response. However, the cabin noise response to high levels of turbulence is different for each of the vehicle geometries. At higher levels of turbulence, the Geometry 1G vehicle shows a quietening effect in the leeward flow region, whereas at lower levels of turbulence, this effect is reversed. Conversely, the Geometry 2G vehicle shows a similar response to both high and low levels of on-road turbulence. This shows that the Geometry 2G vehicle, with modifications to the door mirrors, shows a lower degree of turbulence sensitivity than the Geometry 1G vehicle. Comparing the behaviour of the two vehicle geometries under different flow conditions, shows that shape-change can

THIS DOCUMENT IS PROTECTED BY U.S. AND INTERNATIONAL COPYRIGHT
It may not be reproduced, stored in a retrieval system, distributed or transmitted, in whole or in part, in any form or by any means.
Downloaded from SAE International by Jaguar Cars Ltd, Thursday, August 08, 2013 09:15:34 AM

modify not only noise levels but also sensitivity to on-road turbulence.

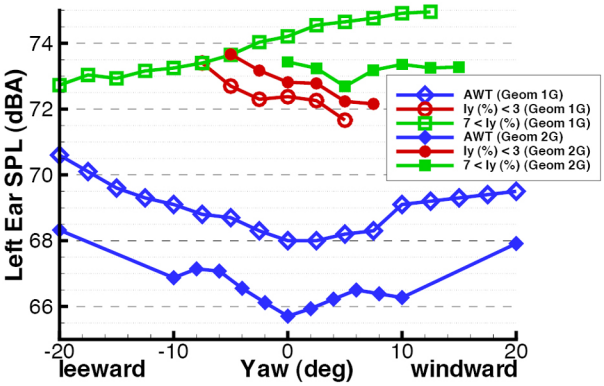

Figure 20. SPL (dBA) sensitivity to yaw and turbulence (Geometry 1G and 2G)

Figure 21 shows the AWT cabin noise response of vehicle Geometry 3G (with bonnet kicker), compared to vehicle Geometry 2G. Vehicle Geometry 3G shows an overall lower SPL for all yaw angles tested in the aeroacoustic wind tunnel, consistent with the findings of Zaccariotto et al. [16]. The increased reduction in cabin noise at windward conditions between zero and ten degrees indicates that the windscreen wipers of the vehicle have greatest effect on the cabin noise under these flow conditions.

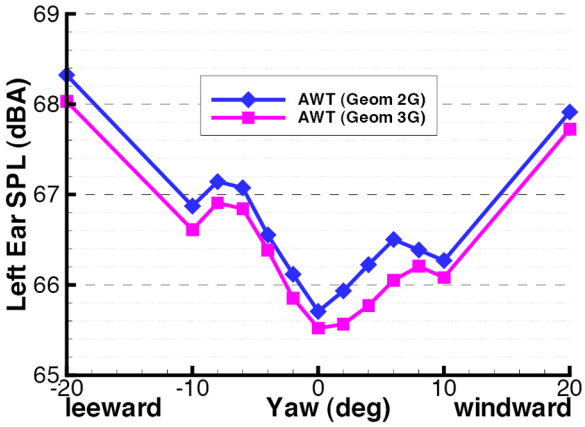

Figure 21. SPL (dBA) sensitivity to yaw (Geometry 2G and 3G)

CONCLUSIONS

Sound pressure levels were measured inside the cabin of a vehicle on-road under a range of conditions and compared against measurements made at the Merkenich aeroacoustic wind tunnel in Cologne at various static yaw angles. Surface pressures and noise from surface microphones in the sideglass region were also recorded on-road. The effects of small geometry changes to the vehicle were also investigated, including a modification to the stem of the door mirror and through the addition of a bonnet kicker.

Sideglass pressures showed close agreement at all turbulence levels whilst surface sound pressure levels also showed similar behaviour under a wide range of on-road flow conditions. While the overall sideglass sound pressure level changed under the various yaw conditions, the change in shape of the frequency spectrum was less significant.

Modifications to the door mirror housing reduced the sensitivity of the in-cabin noise to on-road turbulence, when compared to the base case vehicle. This shows that different geometry vehicles can exhibit difference sensitivities to on-road turbulence. The addition of a kicker to the rear lip of the bonnet also had the effect of slightly reducing in-cabin noise.

REFERENCES

1. Hucho, W.-H., "Aerodynamics of Road Vehicles," SAE International, Warrendale, PA, ISBN 0-7680-0029-7:343, 1998, doi:10.4271/R-177.

2. Blumrich, R., "New Developments in Numerical Vehicle Aeroacoustics," 7th FKFS Conference Progress in Vehicle Aerodynamics and Thermal Management, Stuttgart, 6th July 2009

3. Watkins, S., "Topics in Wind Noise Automobile Wind Noise and its Measurement Part II," SAE International, Warrendale, PA, ISBN 0-7680-0389-X, 1999.

4. George, A.R., "Automobile Aerodynamic Noise," SAE Technical Paper, 900315, 1990, doi: 10.4271/900315.

5. Cogotti, A., "Generation of a Controlled Level of Turbulence in the Pininfarina Wind Tunnel for the Measurement of Unsteady Aerodynamics and Aeroacoustics," SAE Technical Paper, 2003-01-0430, 2003, doi:10.4271/2003-01-0430.

6. Cogotti, A., Cardano, D., Carlino, G., and Cogotti, F., "Aerodynamics and Aeroacoustics of Passenger Cars in a Controlled High Turbulence Flow: Some New Results," SAE Technical Paper, 2005-01-1455, 2005, doi: 10.4271/2005-01-1455.

7. Saunders, J. W. and Mansour, R.B., "On-Road and Wind Tunnel Turbulence and its Measurement Using a Four-Hole Dynamic Probe Ahead of Several Cars," SAE Technical Paper, 2000-01-0350, 2000, doi:10.4271/2000-01-0350.

8. Watkins, S., Riegel, M. and Wiedemann, J. "The Effect of Turbulence on Wind Noise: A Road and Wind-Tunnel Study," 4th International Stuttgart Symposium, FKFS/ Stuttgart University, 20-22nd February 2001. In Automotive and Engine Technology, Expert-Verlag, ISBN 3-8169-1981-2

9. Wordley, S. and Saunders, J., "On-road Turbulence," *SAE Int. J. Passeng. Cars - Mech. Syst.* **1**(1):341-360, 2008, doi: 10.4271/2008-01-0475.

THIS DOCUMENT IS PROTECTED BY U.S. AND INTERNATIONAL COPYRIGHT
It may not be reproduced, stored in a retrieval system, distributed or transmitted, in whole or in part, in any form or by any means.
Downloaded from SAE International by Jaguar Cars Ltd, Thursday, August 08, 2013 09:15:34 AM

10. Wordley, S., and Saunders, J., "On-road Turbulence: Part 2," *SAE Int. J. Passeng. Cars - Mech. Syst.* **2**(1):111-137, 2009, doi:10.4271/2009-01-0002.

11. Krampol, S., Riegel, M. and Wiedemann, J., "Rechnergestuetzte Simulation des Instationaeren Windgeraeusches," ATZ Automobiltechnische, volume 11:111, 2009

12. Lindener, N., Miehling, H., Cogotti, A., Cogotti, F. et al., "Aeroacoustic Measurements in Turbulent Flow on the Road and in the Wind Tunnel," SAE Technical Paper, 2007, doi: 10.4271/2007-01-1551, 2007.

13. Oettle, N., Sims-Williams, D., Dominy, R., Darlington, C. et al., "The Effects of Unsteady On-Road Flow Conditions on Cabin Noise," SAE Technical Paper, 2010-01-0289, 2010, doi:10.4271/2010-01-0289.

14. Lawson, A.A., Dominy, R.G., and Sims-Williams, D.B., "A Comparison Between On-Road and Wind Tunnel Surface Pressure Measurements on a Mid-Sized Hatchback," SAE Technical Paper 2007-01-0898, 2007, doi: 10.4271/2007-01-0898.

15. Lawson, A.A., Sims-Williams, D., B., and Dominy, R.G., "Effects of On-Road Turbulence on Vehicle Surface Pressures in the A-Pillar Region," *SAE Int. J. Passeng. Cars - Mech. Syst.* **1**(1):333-340, 2008, doi:10.4271/2008-01-0474.

16. Zaccariotto, M., Burgade, L. and Chanudet, P., "Aeroacoustic Studies at P.S.A.," 2nd International Stuttgart Symposium, FKFS/Stuttgart University, 18-20th February 1997.

17. Irwin, H., Cooper, K., R. and Girand, R., "Correction of Distortion Effects Caused by Tubing Systems in Measurements of Fluctuating Pressures," *Journal of Industrial Aerodynamics*, **5**(1-2):93-107, 1979

18. Sims-Williams, D.B. and Dominy, R.G., "Experimental Investigation into Unsteadiness and Instability in Passenger Car Aerodynamics," SAE Technical Paper 9800391, 1998, doi: 10.4271/9800391.

19. He, L., "Time Marching Calculations of Unsteady Flows, Blade Row Interaction and Flutter," Von Kármán Institute for Fluid Dynamics, Lecture Series 1996-05, Unsteady Flows in Turbomachines, 1996

CONTACT INFORMATION

Nicholas Oettle
Centre for Automotive Research
School of Engineering and Computing Sciences
Durham University
Durham
DH1 3LE
n.r.oettle@durham.ac.uk

DEFINITIONS AND ABBREVIATIONS

DEFINITIONS

Component turbulence intensity (i = x,y,z)

$$I_i = \frac{\sigma_i}{\bar{U}}$$

Bulk turbulence intensity

$$I = \sqrt{I_x^2 + I_y^2 + I_z^2}$$

ABBREVIATIONS

AWT
Aeroacoustic wind tunnel

HSU
Head and shoulder unit

SPL
Sound pressure level